Start-up procedures and hydraulic characteristics of an innovative controlled double circle anaerobic reactor for treating traditional Chinese medicine wastewater

Longyi Lv*, Weiguang Li*, and Wen Qin*

* School of Municipal and Environmental Engineering, Harbin Institute of Technology, 73 Huanghe Road, Harbin 150090, People Republic of China (E-mail:*llyhit@126.com*; *hitlwg@126.com; qinwenhit@163.com*)

Abstract
In order to verify the feasibility of the innovative controlled double circle anaerobic reactor (CDC) for treating traditional Chinese medicine (TCM) wastewater, the start-up procedures and hydraulic characteristics of the CDC reactor were investigated. The results indicated that within four months, the process of sludge granulation was performed in the CDC reactor by inoculating flocculent sludge for feeding actual TCM wastewater. In the stable stage, the chemical oxygen demand (COD) removal efficiency and biogas production were averagely 95.6% and 0.52 L/gCODremoved, respectively, with an organic loading rate (OLR) of 14.67kg COD m-3 d-1. The hydraulic characteristics of the CDC reactor under different upflow velocities were analyzed using residence time distribution (RTD) method. The results showed that the flow patterns for all test conditions were tend to completely mixed and a negative correlation between the dead space and the upflow velocity was observed. Moreover, the tanks-in-series (TIS) model was more adaptive to simulate the flow characteristics of the CDC reactor than the axial dispersion (AD) model under the present experimental conditions. Therefore, the consistency of the results between performance and hydraulic characteristics proved that the upflow velocity was an important control factor for the CDC reactor to handle the TCM wastewater.

Keywords
Controlled double circle anaerobic reactor; start-up; traditional Chinese medicine wastewater; upflow velocity; residence time distribution

INTRODUCTION

At present, the anaerobic treatment of wastewater, as a sustainable technology, is widely used in the field of industrial wastewater treatment. As a representative of the third-generation of anaerobic reactor, the IC reactor has attracted more and more attention, which has many special advantages such as high OLRs, large height-diameter ratio, land saving, steady operation, resistance to shock loading, and high processing efficiency (Wang et al., 2014). However, the IC reactor has two main technical bottlenecks, which greatly limit its application. First, the IC reactor could quickly start only by the inoculation of granular sludge cultivated by the same or similar waste water, and the seed granular sludge is very expensive. Second, the IC reactor can only be used for high organic concentrations and well biodegradable wastewater such as brewery wastewater, sugar refinery wastewater, citric acid wastewater, and others (Deng et al., 2006; Cui et al., 2011). However, there are a number of industrial wastewater types of poorly biodegradable and even contain toxic materials in real life, such as pharmaceutical wastewater, dyeing wastewater, and others, and the IC reactor is very helpless to these wastewater. This is because that these types of wastewater cannot produce enough biogas to drive liquid circulation, so the mass transfer in the reactor is too low to enable a better removal efficiency.

In recent years, the TCM industry has been rapidly developed because of its unique effectiveness, which results in a correspondingly increase in TCM wastewater production (Su et al., 2015). The composition of TCM wastewater was determined by raw materials and production process, mainly coming from the washing water of raw material, the residual liquid of original medicine and floor washing water (Jiang et al., 2006; Zhao et al., 2007; Chen et al., 2009). The characteristics of TCM wastewater are a complicated composition and a high concentration of natural organic pollutants, such as carbohydrates, alkaloids, phenols, alcohols, amino acid, lignin, proteins, pigments and their hydrolysates (Li et al., 2006). Therefore, TCM wastewater is a kind of high concentration organic wastewater with poor biodegradation, which will cause the serious pollution to the environment if it is not handled. The CDC anaerobic reactor is designed by the authors on the basis of the IC reactor to improve the efficiency of anaerobic biodegradation for industrial wastewater containing high concentrations of organic and toxic substances. The utilization of forced internal & external circulation devices can make up for the IC shortage due to the reduced biogas production during the start-up period, and this makes it possible to start the CDC reactor by inoculating the flocculent sludge. So our first objective is to verify whether the CDC reactor could successfully start-up by inoculating the flocculent sludge for the treatment of actual TCM wastewater at medium temperature range. Specifically, this study was conducted to explore a feasible anaerobic reactor to treat poorly biodegradable and toxic wastewater. The RTD has been an effective hydraulic analysis approach in evaluating the mixing pattern (plug flow or completely mixed) and the dead space distribution due to its advantages, such as simple experimental method and wide application (Li et al., 2015). In this study, a series of RTD studies of the CDC reactor was performed to investigate hydraulic characteristics to illustrate that the variance of the upflow velocity (V_{up}) affected the mixing pattern and dead space. Our second objective is to analyze the flow pattern and dead space of the CDC reactor to guarantee a more successful biological process.

MATERIAL AND METHODS

Experimental equipment

A schematic diagram of the CDC anaerobic reactor modified from the traditional IC anaerobic reactor is shown in Figure 1. The CDC reactor was made of a polymethyl methacrylate column with a height of 1750 mm and effective volume of 7.5 L.The CDC reactor from bottom to top was also divided into four parts: 1st reaction area, 2nd reaction area, precipitation area and gas–liquid separation area, whose effective volume were 2.4 L, 4.0L, 1.1L and 1.60L respectively. The CDC reactor was equipped with an external circulation downcomer, which was used to complete the cycle of the second reaction zone. And the CDC reactor was assembled the internal & external circulation conversion devices, which were composed of the switching valves set for the conversion between automatic operation mode and forced operation mode of internal & external circulation system. The CDC reactor was operated at 35±1℃, which was controlled by a thermostat.

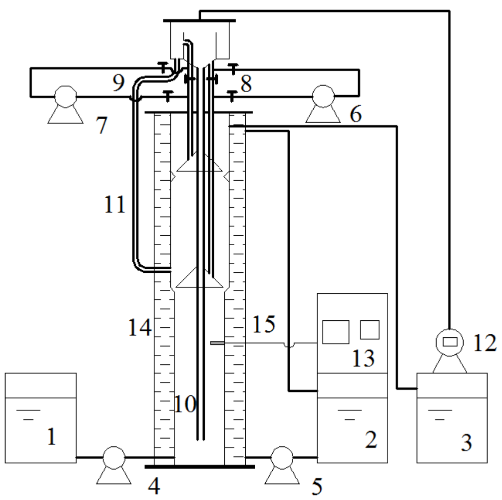

Fig. 1. Schematic diagram of the DC anaerobic reactor. 1 – Influent tank. 2 – Thermostatic water bath. 3 – Effluent tank. 4 – Influent peristaltic pump. 5 – Hot water circulation peristaltic pump. 6 – Forced internal circulation peristaltic pump. 7 – Forced external circulation peristaltic pump. 8 – Internal circulation conversion device. 9 – External circulation conversion device. 10 – Internal circulation downcomer. 11 – External circulation downcomer. 12 – Wet gas meter. 13 – Control cabinet. 14 – Heat preservation jacket. 15 – Temperature probe.

Sludge inoculation and experimental wastewater

Flocculent sludge for inoculation was obtained from the sludge thickener of a TCM factory (Hubei, China). The seeds were inoculated to 30% of the reactor volume, and its SS concentration was 14.8 g L^{-1}. Actual TCM wastewater that collected from the effluent of a TCM factory (Hubei, China) was used in the start-up procedures of the CDC reactor. The raw TCM wastewaters were characterized by a high COD (6000–20,000 mg L^{-1}), a low BOD_5/COD ratio (approximately 25%) and a low pH (3-6). Sodium bicarbonate was used to adjust the feed water to pH 6.5–7.5 and increase its alkalinity. Urea and potassium dihydrogen phosphate were added to regulate the value of COD: N: P to be about 250:5:1 throughout the experimental process. To ensure a good environment for the growth of microorganisms, micronutrients such as iron, calcium, manganese, magnesium, and some trace minerals were added in the TCM wastewater (Su et al., 2015).

Reactor start-up procedures

The start-up process in the DC reactor was performed in three stages, which is shown in Table 1. The stage (a) was HRT-shortening stage including three periods(1-3), in which the hydraulic retention time (HRT) of DC reactor was shortened gradually (36h, 24h, 18h) with the concentration of influent COD constant (3000mg L^{-1}). The stage (b) was concentration-increase stage including five periods(4-8), in which the HRT of DC reactor was 18h, and the concentration of influent COD were 5000, 7000, 9000, 11000, 13000 mg L^{-1} respectively. The stage (c) was operation-stabilization stage including one period (9), in which the HRT of DC reactor was 18h and the concentration of influent COD was 1100 mg L^{-1}. In the period 1-8, the OLR was increased from 2-17.33 kg COD m^{-3} d^{-1}, while the OLR was kept constant 14.67 kg COD m^{-3} d^{-1} in the period 9.

Analytical methods

COD, BOD_5 were analysed according to the Standard Methods (APHA, 2005). The volume of the biogas was determined using a wet gas flow meter. A series of RTD experiments was conducted under different upflow velocity conditions shown in Table 2. Sodium chloride was employed as the tracer because sodium ions and chloride ions were not absorbed by sludge particles, and had no inhibitory effects on anaerobic bacteria at low concentrations (Tomlinson and Chambers, 1979; Anderson et al., 1991; Asraf-Snir and Gitis, 2011; Li et al., 2016). To acquire the RTD curves, 50 mL sodium chloride solution (3932 mg Na^+/Na) was instantly injected prior to the inlet, then the effluent samples were collected regularly from the outlet of the reactor for detecting the concentration of sodium ion, and the total sampling time was four times the nominal HRT. The concentration of sodium ion (Na^+) was monitored by a sodium ion concentration detector (Shanghai, China), which could detect the concentration of sodium ion through measuring electromotive force formed by the sodium electrode and the reference electrode.

Table 1 The start-up procedures of CDC reactor.

	stage (a)			stage (b)					stage (c)
Period	1	2	3	4	5	6	7	8	9
Day(d)	1-30	31-44	45-60	61-75	76-94	95-105	106-116	117-125	126-215
Influent COD (mg L^{-1})	3000	3000	3000	5000	7000	9000	11000	13000	11000
HRT (h)	36	24	18	18	18	18	18	18	18
OLR (kg COD m^{-3} d^{-1})	2	3	4	6.67	9.33	12	14.67	17.33	14.67
$V_{up}1$(m h^{-1})	0.59	0.89	0.89	2.01	2.01	2.01	3.03	3.03	3.03
$V_{up}2$(m h^{-1})	0.16	0.31	0.31	0.50	0.50	0.50	0.79	0.79	0.79

Table 2 The results of tracer tests and main hydrodynamics parameters values of different flow models.

Run No.	$V_{up}1$ (m h^{-1})	$V_{up}2$ (m h^{-1})	HRT(h)	$\bar{t}$ (h)	σ^2	V_d(%)	AD model		TIS model	
							D/uL	MSPE	N	MSPE
1	0.89	0.31	24	20.96	0.27	12.7	0.140	0.0466	3.7	0.0057
2	2.01	0.50	24	22.46	0.37	6.4	0.194	0.0468	2.7	0.0019
3	3.03	0.79	24	23.08	0.51	3.8	0.273	0.0669	2.1	0.0018

Modelling and evaluation of models

RTD is obtained by measuring the actual residence time of liquid cell in the reactor. Flow models are determined through the analysis of RTD function, optimum flow model is then selected by model fitting effect.

RTD function

The exit-age distribution function *E* (*t*) was calculated using Eq. (1) (Levenspiel, 1999):

$$E(t) = \frac{C(t)}{\int_0^\infty C(t)dt} \tag{1}$$

where, *t* was time, hr; *C* (*t*) was the tracer concentration at time *t*, mg L^{-1}.

$$\bar{t} = \frac{\int_0^\infty tC(t)dt}{\int_0^\infty C(t)dt} = \int_0^\infty tE(t)dt\,;\ \sigma_t^2 = \frac{\int_0^\infty (t-\bar{t})^2 C(t)dt}{\int_0^\infty C(t)dt} = \int_0^\infty t^2\,E(t)dt - (\bar{t})^2 \tag{2}$$

Eq. (2) was used to calculate the mean residence time ($\bar{t}$) and distribution variance (σ_t^2).

To compare the mixing patterns at different HRTs, the unit of time was normalized. The normalized time θ and normalized concentration *E* (θ) were given by:

$$\theta = \frac{t}{HRT};\ E(\theta) = \frac{C(\theta)}{C_0} \tag{3}$$

in which $C(\theta)$ was the tracer concentration at normalized time θ, mg L^{-1}; C_0 was the initial tracer concentration, mg L^{-1}.

The dead space (V_d, %) was calculated using Eq. (4) as follows:

$$V_d = \left(1 - \frac{\bar{t}}{HRT}\right) \times 100\% \tag{4}$$

Axial dispersion model

AD considering the axial motion of fluid element was first used by Danckwerts (Danckwerts, 1953). The basic one-dimensional partial differential equation representing axial dispersion model was:

$$\frac{\partial E(\theta)}{\partial \theta} = \left(\frac{D}{uL}\right)\frac{\partial^2 E(\theta)}{\partial z^2} - \frac{\partial E(\theta)}{\partial z} \tag{5}$$

where D was the axial dispersion coefficient, m^2 s^{-1}; u is the velocity, m s^{-1}; z is dimensionless and defined as the ratio of the axial position to the reactor length L. The analytical solution for Eq. (5) was given in a dimensionless form as follows:

$$E(\theta) = \frac{1}{2\sqrt{\pi(\frac{D}{uL})\theta}} exp\left[-\frac{(1-\theta)^2}{4\theta(\frac{D}{uL})}\right] \tag{6}$$

According to closed boundary condition, $\frac{D}{uL}$ could be calculated by using Eq. (7).

$$\sigma^2 = 2\left(\frac{D}{uL}\right) - 2\left(\frac{D}{uL}\right)^2\left(1 - e^{-uL/D}\right) \tag{7}$$

Pe was the dimensionless Peclet number, which was the reciprocal of *D/uL* can be calculated as Eq. (8):

$$\sigma^2 = \left(\frac{2}{Pe}\right) - 2\left(\frac{1}{Pe}\right)^2 (1 - e^{-Pe}) \quad (8)$$

Pe could be used to characterize the axial back-mixing. The larger was the value of Pe, the weaker was the back-mixing (Ji et al., 2012). σ^2 was the dimensionless variance of RTD, $\sigma^2 = \sigma_t^2/\bar{t}^2$.

Tanks-in-series model

TIS is applied when a large degree of back-mixing. The exit-age distribution function $E(\theta)$ could be described as follows (Ji et al., 2012):

$$E(\theta) = \frac{N^N}{(N-1)!}\theta^{N-1}e^{-N\theta} \quad (9)$$

where N was the number of tanks-in-series, could be calculated as Eq. (10):

$$\sigma^2 = \frac{1}{N} \quad (10)$$

As the value of N tends to 1, the flow pattern of the reactor approaches that of being completely mixed. While, as N tends to ∞, the flow pattern of the reactor approaches that of plug flow.

Evaluation of models

Mean squared error of prediction (MSPE) as a criterion for evaluating and comparing alternative models was first proposed by Wallach and Goffinet (Wallach and Goffinet, 1989). In order to compare the accuracy of alternative flow models, MSPE could be defined as follows:

$$MSPE = \frac{1}{N}\sum_{i=1}^{N}(E_i - M_i)^2 \quad (11)$$

where N was the data number, E_i was the i-th observed value by the RTD experiment and M_i was the corresponding model prediction.

RESULTS AND DISCUSSION

Treatment effect

COD removal. COD was used as an important parameter in order to assess the performance of anaerobic reactors (Bertolino et al., 2012). Start-up of the CDC anaerobic reactor was accomplished by a stepped increase of the OLR, which could be achieved by shortening the HRT (stage (a)) or increasing the influent concentration (stage (b)). The changes in the influent/effluent COD concentration and COD removal efficiency of the CDC anaerobic reactor for the treatment of actual TCM wastewater during the whole start-up process are shown in Fig. 2.

As shown in Fig. 2, the COD removal efficiency was substantially increasing in stage (a). During the initial 15 days in period 1(P1), the effluent COD concentration was always kept over 1000 mg L^{-1} and the COD removal rate was less than 60%. This finding indicated that it took a period of time to adapt to a new environment for the flocculent seed sludge, and then better removal was achieved rapidly after the seed sludge acclimatization to its new surroundings in the later 15 days of P1. When the COD removal rate reached more than 85%, the HRT was shortened from 36h (P1) to 24h (P2) at day 31, and the COD removal efficiency dropped dramatically from 87.1 to 65.2%. After the recovery of 14 days, the COD removal rate gradually increased to 85% and the effluent COD concentration was less than 400 mg L^{-1}(P2). In P3, 16 days were used to increase the COD removal efficiency from 57.7 to 87.2%, which was caused by the shortening of HRT from 24 (P2) to 18h (P3).

In stage (b), the HRT was maintained at 18h and the concentrations of influent COD were roughly 5000(P4), 7000(P5), 9000(P6), 11000(P7), 13000(P8) mg L^{-1} respectively, which resulted in corresponding OLRs of 6.67, 9.33, 12, 14.67, 17.33 kg COD m^{-3} d^{-1} respectively. In periods 4–7, the fluctuations of influent load could cause the COD removal rate decreasing sensitively then recovering gradually. However, the COD removal rate could not be restored and the effluent COD concentration was kept over 2200 mg L^{-1} in P8. The results showed that the OLR of 17.33 kg COD m^{-3} d^{-1} had reached the maximum degradation limit of the CDC anaerobic reactor.

In stage (c), the influent COD concentration was maintained at 11,000 mg L^{-1} summarily and the HRT was kept constant 18h, which was equivalent to OLR of 14.67 kg COD m^{-3} d^{-1}. The CDC anaerobic reactor reached steady state after day 141. The COD removal efficiency remained around 95%, while the COD concentration in effluent was about 450 mg L^{-1} in the CDC anaerobic reactor. The results confirmed that the CDC anaerobic reactor was feasible for the anaerobic biodegradation of the high strength TCM wastewater. Our previous study examined the performance of the EGSB reactor for treating TCM wastewater, the results showed that: once the OLR exceeded 13.00 kg COD m^{-3} d^{-1}, the COD removal efficiency would decrease to approximately 78% and the effluent COD concentration was over 1000 mg L^{-1}. This comparison showed that the CDC reactor was more effective for treating TCM wastewater. The reasons for this effectiveness were that the mass transfer efficiency between granular sludge and waste water was enhanced by the forced internal & external circulation system, and the CDC reactor provided a good growth environment for methane-producing bacterial by added external circulation device.

Biogas production. Biogas production can directly reflect the number and activity of methanogenic bacteria, thereby affecting the operation conditions of an anaerobic reactor (Badshah et al., 2012). Curves of biogas production, OLR and upflow velocity in the CDC reactor with time are shown in Fig. 3.

In stage (a), the yield of biogas increased slowly from 0.10 to 8.65 L $d^{-1}$with the increasing OLR. This was because that a period of time was needed for the flocculent seed sludge to adapt to a new growth environment, and methanogens grew slowly with a long generation time. Such a low yield of biogas was insufficient to drive internal & external circulation flow, so the internal & external circulation forced system were employed to ensure a proper upflow velocity for screening of granular sludge. The upflow velocity in the 1st reaction area ($V_{up}1$) of the CDC reactor increased stepwise from 0.59 to 0.89 m h^{-1} with the increasing OLR while the upflow velocity in the 2nd reaction area ($V_{up}2$) was increased from 0.16 to 0.31 during the stage (a). $V_{up}2$ was lower than $V_{up}1$, which was due to the smaller particle size of sludge in the second reaction zone, and lower upflow velocity could avoid a large loss of granular sludge. The utilization of high upflow velocities is reported as a good strategy to promote the formation of granular sludge (Pol et al., 2004; Jin et al., 2012). The granulation process does not occur due to the lack of selection of good settling biomass at lower upflow velocities (Val Del Río et al., 2015).Therefore, the upflow velocity is an important parameter during the start-up phase of anaerobic reactors.

In stage (b), the yield of biogas in the CDC reactor increased from 13.45 to 58.00 L d^{-1} with the OLR increasing from 6.67 to 17.33 kg COD m^{-3} d^{-1}. As the granular sludge gradually formed and the increasing OLR, the biogas production quickly increased. This phenomenon was more pronounced after day 107, and this was because that $V_{up}1$ increased to 3.03 and $V_{up}2$ increased to 0.79, which enhanced the mixture effect between wastewater and sludge and reduced the dead zone of the CDC reactor. Therefore, the upflow velocity was higher, which caused a further increase in the biogas production and removal efficiency.

The OLR reduced to 14.67 kg COD m^{-3} d^{-1} in stage (c). A rapid decline of the yield of biogas was obtained at the beginning of stage (c), and followed by a slow increase, which is consistent with COD removal efficiency in that time. These results indicated that excessive influent impact load could cause the activity of methanogenic bacteria to be inhibited, and the recovery was slow. After day 147, the yield of biogas was stabilized, and the biogas production exceeded 55 L d^{-1}. In order to reduce the energy consumption of the system due to liquid pumping, the internal circulation adopted gas-lift automatic operation mode by the conversion devices of the CDC reactor after day 180. The external circulation forced system was still employed as inadequate biogas production did not have enough power to lift wastewater mixed with sludge in the 2nd reaction area. During day 180-215, the average yield of biogas was 57.12 L d^{-1}, which was equivalent to 0.52 L biogas per g $COD_{removed}$. The result indicates that higher methane yield could still be guaranteed by gas-lift circulation in the 1st reaction area of CDC reactor.

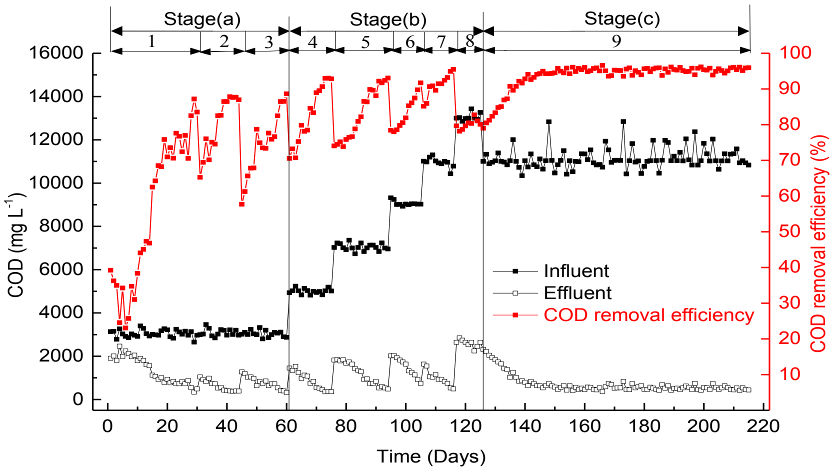

Fig. 2. Variations in the influent/effluent COD concentration and COD removal efficiency.

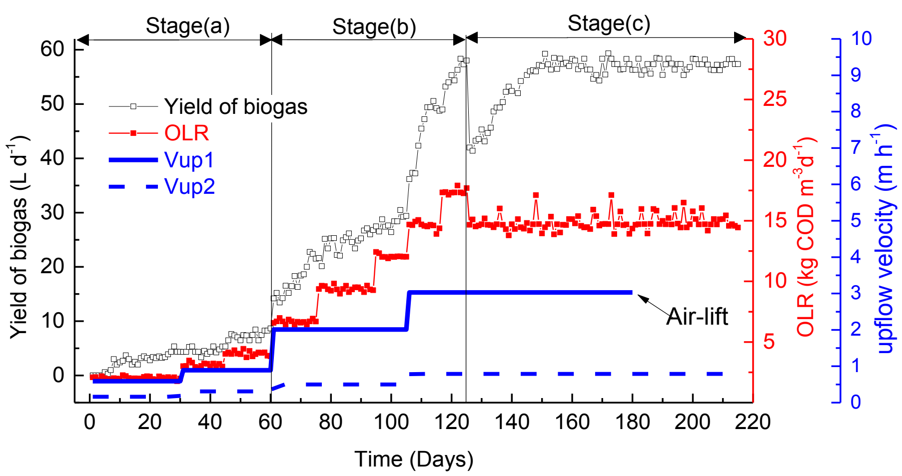

Fig. 3. Changes in the biogas production, OLR and upflow velocity.

Hydraulic characteristics

RTD experiment. As shown in Fig. 4, the shapes of $E(\theta)$ - θ curve are the same at different runs: the value of $E(\theta)$ increases until a maximum value from zero and then gradually reduced to zero. These curves are dome-shaped, which is consistent with previous studies(Levenspiel, 1999; Ji et al., 2012). With the increase of upflow velocity, the maximum tracer concentration and the time to reach the peak concentration were gradually decreased. The E-curves of different upflow velocities showed prolonged tails, and the tail at a high upflow velocity was steeper than that at a low upflow velocity. Most of the tracer left the reactor before θ = 1.0 at all runs, which indicated that there were dead spaces (or short-circuits) in the CDC reactor(Singh et al., 2006).

Dead space. The dead space is a region in the reactor where liquid does not flow or flow slowly, and it can reduce the effective volume of the reactor. The total dead space can be divided into the categories of hydraulic dead space and biological dead space. Hydraulic dead space is related to the upflow velocity and the internal structure of the reactor, and biological dead space is related to the biomass concentration and activity(Young and Young, 1988; Li et al., 2016). The total dead space (V_d) was calculated using Eq. (4), and the result was shown in Table 2. The values of total dead space caused by upflow velocity were 12.7%, 6.4% and 3.8% respectively at a Low, medium and high upflow velocity. The result indicated the upflow velocity had a significant effect on the dead space, and a higher upflow velocity could lead to a smaller dead space. These results were mainly because at a high upflow velocity, the mass transfer of biomass and wastewater was strengthened and more gas would be released, the flow rate and gas flow velocity in the reactor were sufficient enough to disturb the sludge bed and avoid channelling, thus creating less dead space(Li et al., 2015). Compared with some of the previous studies (Torres et al., 2000; Peña et al., 2006; Bhattacharyya and Singh, 2010; Sarathai et al., 2010), the CDC reactor showed a much smaller dead zone at all runs and it could be concluded that the CDC reactor was able to provide a larger effective volume than those reported reactors due to its configuration.

Non-ideal flow model adjustment. The AD and the TIS models were applied to fit the E-curves. The hydrodynamic parameters were obtained according to the experimental results, as shown in Table 2. In the AD model, axial dispersion degrees (D/uL) ranging from 0.140 to 0.273, indicating that the flow pattern has a significant tendency to complete mixing(Levenspiel, 1999). As shown in Figure 5, the value of D/uL increased with the increase of upflow velocity. This changing trend indicated a greater degree of back-mixing as the increase of upflow velocity because higher flow rate could cause more small vortexes, which increased the turbulence of the flow. The MSPE of AD model gradually increased with the increase of upflow velocity shown in Table 2, which argued that the lower upflow velocity, the better simulation result by using the AD model. But the MSPE of AD model was much higher than the MSPE of TIS model at all runs, which indicated that the TIS model was more adaptive to simulate the flow pattern characteristics of the CDC reactor than the AD model under the present experimental conditions.

The TIS model was characterized by N. When $N \leqslant 3$ the flow was considered completely mixed(Ji et al., 2012). According to the values of N in Table 2, the back-mixing predicted by the TIS model showed the same trend as that predicted by the AD model. As shown in Figure 5, the value of N decreased with the increase of upflow velocity. The finding indicated that the higher upflow velocity, the flow pattern of the reactor was closer to that of being completely mixed. The higher upflow velocity was, the closer the value of N fitted the number of actual reaction zones (two areas) of the CDC reactor. The interpretation of this phenomenon was that the first three phase separator in the CDC reactor inhibited back-mixing between the 1st and 2nd reaction area; however, significant mixing due to the recirculation within each individual reaction area was observed. Therefore, the CDC reactor is equivalent to two continuous stirred tank reactors (CSTRs) in series together in the vertical direction in the case of high upflow velocity. For the MSPE of TIS model, the TIS model showed good fitting effect, which was shown in Figure 8, and the best adjustment of the experimental data was fitted to the TIS model with $V_{up}1$ of 3.03 m/hr and $V_{up}2$ of 0.79 m/hr.

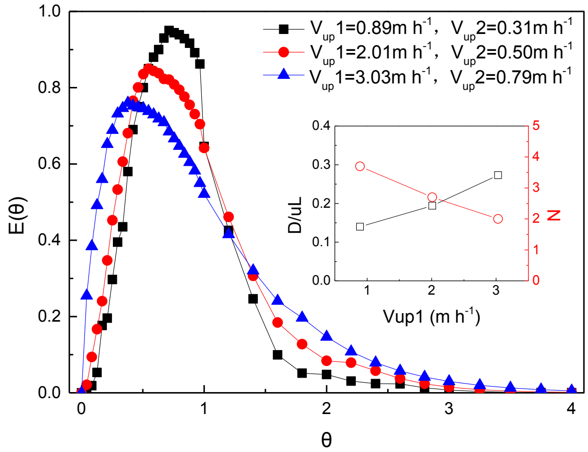

Fig. 4. The E-curves of different upflow velocities and values of D/uL and N for each upflow velocity.

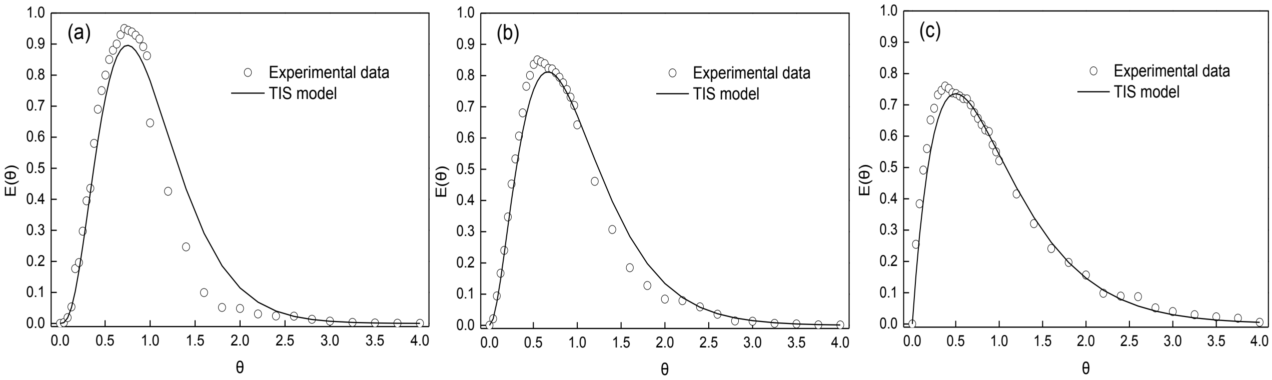

Fig. 5. Simulated and measured tracer concentrations for the CDC reactor under different upflow velocities conditions: (a) run 1, $V_{up}1$=0.89 m h^{-1}, $V_{up}2$=0.31 m h^{-1}; (b) run 2, $V_{up}1$=2.01 m h^{-1}, $V_{up}2$=0.50 m h^{-1}; (c) run 3, $V_{up}1$=3.03 m h^{-1}, $V_{up}2$=0.79 m h^{-1}.

CONCLUSIONS

This study investigated the possibility of applying the CDC reactor to treat TCM wastewater, and the flow characteristics in the CDC reactor were analysed. The research results confirmed that the CDC reactor was feasible for the anaerobic biodegradation of actual TCM wastewater, and the CDC reactor could be successfully started up by the inoculation of flocculent sludge in four months. The CDC reactor demonstrated a good COD removal of 95% and a high biogas yield of 0.52 L/gCOD$_{removed}$ with an OLR of 14.67kg COD m^{-3} d^{-1} in the stable stage. Additionally, the flow pattern of the CDC reactor tended to the completely mixed for all test conditions, and the trend was more obvious at higher upflow velocity. The CDC reactor showed a smaller dead space with a higher upflow velocity, and a large effective volume could be provided due to its configuration. The hydrodynamics assessment of the CDC reactor demonstrated that the TIS model was a better fit for the experimental data compared with the AD model.

ACKNOWLEDGMENT

This work was financially supported by the National Science and Technology Major Project of China [No. 2012ZX07205002].

REFERENCES

Anderson, G.K., Campos, C., Chernicharo, C., Smith, L.C., 1991. Evaluation of the inhibitory effects of lithium when used as a tracer for anaerobic digesters. WATER RES 25, 755-760.

APHA, A.W., 2005. Standard methods for the examination of water and wastewater.

Asraf-Snir, M., Gitis, V., 2011. Tracer studies with fluorescent-dyed microorganisms—A new method for determination of residence time in chlorination reactors. CHEM ENG J 166, 579-585.

Badshah, M., Parawira, W., Mattiasson, B., 2012. Anaerobic treatment of methanol condensate from pulp mill compared with anaerobic treatment of methanol using mesophilic UASB reactors. BIORESOURCE TECHNOL 125, 318-327.

Bertolino, S.M., Rodrigues, I.C., Guerra-Sá, R., Aquino, S.F., Leão, V.A., 2012. Implications of volatile fatty acid profile on the metabolic pathway during continuous sulfate reduction. J ENVIRON MANAGE 103, 15-23.

Bhattacharyya, D., Singh, K.S., 2010. Understanding the mixing pattern in an anaerobic expanded granular sludge bed reactor: effect of liquid recirculation. J ENVIRON ENG 136, 576-584.

Chen, Z., Hu, D., Zhang, Z., Ren, N., Zhu, H., 2009. Modeling of two-phase anaerobic process treating traditional Chinese medicine wastewater with the IWA Anaerobic Digestion Model No. 1. BIORESOURCE TECHNOL 100, 4623-4631.

Cui, P., Zhou, X., Zhang, Y., 2011. The Feasibility Study of Cotton Pulp Wastewater Treatment with IC Anaerobic Reactor. Procedia Environmental Sciences 11, 686-692.

Danckwerts, P.V., 1953. Continuous flow systems: distribution of residence times. CHEM ENG SCI 2, 1-13.

Deng, L.W., Zheng, P., Chen, Z.A., 2006. Anaerobic digestion and post-treatment of swine wastewater using IC–SBR process with bypass of raw wastewater. PROCESS BIOCHEM 41, 965-969.

Ji, J., Zheng, K., Xing, Y., Zheng, P., 2012. Hydraulic characteristics and their effects on working performance of compartmentalized anaerobic reactor. BIORESOURCE TECHNOL 116, 47-52.

Ji, J.Y., Zheng, K., Xing, Y.J., Zheng, P., 2012. Hydraulic characteristics and their effects on working performance of compartmentalized anaerobic reactor. BIORESOURCE TECHNOL 116, 47-52.

Jiang, B., Lu, X., Liu, Z., Ge, J., Gui, Y., 2006. Application of reactor theory to technical reformation works for traditional Chinese medicine wastewater treatment. Technology of Water Treatment 32, 86-88.

Jin, X., Wang, F., Liu, G., Yan, N., 2012. A key cultivation technology for denitrifying granular sludge. PROCESS BIOCHEM 47, 1122-1128.

Levenspiel, O., 1999. Chemical Reaction Engineering. third ed. John Wiley and Sons, New York.

Li, D.W., Li, D., Wang, K.H., Yang, J., Yuan, X., 2006. Wastewater treatment of traditional Chinese medicine by two phase anaerobic. Technology of Water Treatment (China) 32, 81-83.

Li, S., Nan, J., Gao, F., 2016. Hydraulic characteristics and performance modeling of a modified anaerobic baffled reactor (MABR). CHEM ENG J 284, 85-92.

Li, S., Nan, J., Li, H., Yao, M., 2015. Comparative analyses of hydraulic characteristics between the different structures of two anaerobic baffled reactors (ABRs). ECOL ENG 82, 138-144.

Peña, M.R., Mara, D.D., Avella, G.P., 2006. Dispersion and treatment performance analysis of an UASB reactor under different hydraulic loading rates. WATER RES 40, 445-452.

Pol, L.H., de Castro Lopes, S.I., Lettinga, G., Lens, P., 2004. Anaerobic sludge granulation. WATER RES 38, 1376-1389.

Sarathai, Y., Koottatep, T., Morel, A., 2010. Hydraulic characteristics of an anaerobic baffled reactor as onsite wastewater treatment system. 环境科学学报:英文版 22, 1319-1326.

Singh, K.S., Viraraghavan, T., Bhattacharyya, D., 2006. Sludge blanket height and flow pattern in UASB reactors: Temperature effects. J ENVIRON ENG 132, 895-900.

Su, C., Li, W., Wang, K., Li, Y., 2015. Start-up procedures and analyses of sludge characteristics in a novel double circle anaerobic reactor for treating traditional Chinese medicine wastewater. ENVIRON TECHNOL 36, 1529-1537.

Tomlinson, E.J., Chambers, B., 1979. Effect of longitudinal mixing on the settleability of activated sludge. WRC.

Torres, J.J., Soler, A., Sáez, J., Llorens, M., 2000. Hydraulic performance of a deep stabilisation pond fed at 3.5 m depth. WATER RES 34, 1042-1049.

Val Del Río, A., Buys, B., Campos, J.L., Méndez, R., Mosquera-Corral, A., 2015. Optimizing upflow velocity and calcium precipitation in denitrifying granular systems. PROCESS BIOCHEM 50, 1656-1661.

Wallach, D., Goffinet, B., 1989. Mean squared error of prediction as a criterion for evaluating and comparing system models. ECOL MODEL 44, 299-306.

Wang, J., Xu, W., Yan, J., Yu, J., 2014. Study on the flow characteristics and the wastewater treatment performance in modified internal circulation reactor. CHEMOSPHERE 117, 631-637.

Young, H.W., Young, J.C., 1988. Hydraulic Characteristics of Upflow Anaerobic Filters. J ENVIRON ENG 114, 621-638.

Zhao, Z., Mingqing, T., Qikai, N., Kui, Y., Baosheng, C., Haijing, L., Guoming, L., 2007. The practice on engineering treatment of Chinese traditional medicine wastewater. China Resources Comprehensive Utilization 25, 19-21.